Structure of the low-lying 2^+ states in ^{14}C from inelastic pion scattering

A. C. Hayes, S. Chakravarti,* D. Dehnhard, P. J. Ellis, D. B. Holtkamp,†
L.-P. Lung, and S. J. Seestrom-Morris†
University of Minnesota, Minneapolis, Minnesota 55455

Helmut Baer and C. L. Morris
Los Alamos National Laboratory, Los Alamos, New Mexico 87545

S. J. Greene†
New Mexico State University, Las Cruces, New Mexico 88003

C. J. Harvey‡
University of Texas, Austin, Texas 78712
(Received 16 December 1987)

Differential cross sections for inelastic pion scattering from ^{14}C measured at $T_\pi = 164$ MeV, for the 2^+_1 and 2^+_2 states and an unresolved peak at 10.4 MeV, were analyzed by distorted-wave impulse approximation and coupled-channel calculations using transition densities derived from large scale shell model calculations. The pion and $B(E2)$ data showed strong quenching of the isovector component for the 2^+_1 transition, which required different effective charges for the p and sd shells. The pion data for the 2^+_2 are an order of magnitude smaller than for the 2^+_1 state, and this was understood in terms of strong cancellations between the neutron and proton transition amplitudes. This transition was found to be very sensitive to details of the calculations. The 10.4 MeV data were consistent with the excitation of a 3^- state.

I. INTRODUCTION

In a simple shell model the lowest positive parity states of ^{14}C consist of two proton holes in the p shell. However, it is well known[1-3] that to explain the two $J^\pi = 2^+$ states at 7.01 and 8.32 MeV, it is necessary to consider 2p-4h core excitations. Extended shell model calculations[4,5] predict that such $2\hbar\omega$ configurations play a significant role in the low-lying spectrum of ^{14}C. In the case of these two 2^+ states, the dominantly neutron $|(p^{-4})(sd)^2\rangle$ excitations are strongly mixed with the pure proton $|(p^{-2})\rangle$ configurations, whereas for the $J^\pi = 0^+$ ground state core-excitations are predicted to make up about 4–17 % of the wave function. The unique ability of pions, at energies close to the (3,3) resonance, to identify neutron versus proton excitations of the nucleus makes pion inelastic scattering an ideal probe to study the configuration mixing in these states and to test large shell model calculations.

The most surprising feature of the inelastic pion scattering data[6,7] for the 2^+ states of ^{14}C is the observed near equality of the π^+ and π^- cross sections to the 2^+_1(7.01 MeV) state. In a simple p-shell calculation we expect the cross-section ratio to be close to 9:1, while for large extended shell model calculations we find the predicted ratio is slightly less than 2:1. Another interesting feature of the (π,π') data is the clear evidence for strong destructive interference between the p-shell (proton) and sd-shell (neutron) amplitudes to the 2^+_2(8.32 MeV) state. The π^+ cross section to this state is observed to be about an order of magnitude smaller than that to the 2^+_1(7.01

MeV) state, and these cancellations are even more dramatic for the π^- cross sections.

In the present work we present distorted wave impulse approximation (DWIA) and coupled-channel (CC) analyses of inelastic pion scattering to the 2^+ states in ^{14}C. The transition densities used were derived from a large $(0+2\hbar\omega)$ shell model calculation. Detailed analysis of the (π,π') data within our model suggests that the near equality of $\sigma(\pi^+)$ and $\sigma(\pi^-)$ for the 2^+_1(7.01 MeV) state is evidence for the need for different effective polarization charges for the p shell and sd shell. In the case of the 2^+_2(8.32 MeV) state both the predicted cross-section magnitude and the shape of the angular distribution are found to be very sensitive to small components in the wave function. Channel couplings between the $(0^+_1, 2^+_1, 2^+_2)$ states increase the predicted (π,π') cross sections to the 2^+_2 level and slightly improve the $\sigma(\pi^+)/\sigma(\pi^-)$ ratio to the 2^+_1 level.

Another peak is observed at 10.4 MeV. Near this excitation energy three states are known[8] with spin and parity assignments $(3^-)(10.43$ MeV$)$, $2^+(10.45$ MeV$)$, and $\geq 1(10.50$ MeV$)$. The DWIA predictions for the 2^+_2 state are a factor of 10 (100) smaller than the π^+ (π^-) data. However, a shell model calculation of Kurath[9] predicts a 3^- state near 10.4 MeV and DWIA results for this theoretical 3^- state are in good agreement with the data for the 10.4 MeV peak.

The experiment, which was carried out at the Energetic Pion Channel and Spectrometer (EPICS) (Ref. 10) at the Clinton P. Anderson Meson Physics Facility (LAMPF), has been discussed elsewhere.[6,12] It is neces-

sary to point out, however, that a measurement[11] of the target composition requires that the preliminary cross sections reported in Refs. 6 and 7 be increased by a factor of 1.25. In Sec. II we present the shell model basis chosen for ^{14}C and in Sec. III we compare the results of the DWIA analysis with our experimental data. We discuss the role of effective charges in pion inelastic scattering and give the results of the CC calculations. In Sec. V we present our concluding remarks.

II. SHELL MODEL CALCULATIONS

There have been extensive shell model calculations[4,5] for the $A = 14$ system, which have been quite successful in reproducing the excitation energies and the known electromagnetic strengths between the low-lying states. For the positive parity states of ^{14}C it is important to include both $0\hbar\omega$ and $2\hbar\omega$ excitations, but Lie[4] found 4p-6h $4\hbar\omega$ configurations to be unimportant for the low-lying spectrum. The mixing of the dominantly 2p-4h $2\hbar\omega$ and the p^{-2} $0\hbar\omega$ configurations in the wave functions of these low-lying states is not accurately known and can be difficult to calculate, especially when the states involved are closely spaced in energy. However, it is to this configuration mixing that inelastic pion scattering studies are particularly sensitive.

The present shell model calculations are performed in an SU(3) basis. States which correspond to spurious center of mass (c.m.) motion have been exactly removed from the basis. We use a complete $0\hbar\omega$ and a large $2\hbar\omega$ basis which includes the dominant $s^4p^8(sd)^2$ and $s^4p^9(pf)$, configurations. Our $2\hbar\omega$ basis is very similar to that used in Ref. 5 and includes the SU(3) configurations with $(\lambda,\mu)=(4,4)$, (5,2), (2,5), (4,1), (1,4), (3,3), (6,0), and (0,6). We have not included all possible (λ,μ) values for the $2\hbar\omega$ configurations as this would involve an unreasonably large basis; the omitted configurations being all those with $(\lambda,\mu)=(2,2)$, (3,0), (0,3), (1,1), and (0,0). Apart from the (2,2) representation, these configurations would yield only very small components in the low-lying 0^+ and 2^+ wave functions and these are not important for pion scattering. With regard to the (2,2) representation, Kozub et al.[5] did include it in their study of electromagnetic transitions involving a change of parity since it can be important in calculating $E1$ transitions. There are however two interrelated difficulties associated with the (2,2) representation. Firstly, it couples to the $0\hbar\omega$ configurations via $\Delta\hbar\omega=2$ matrix elements which transform as $(\lambda,\mu)=(2,0)$ under SU(3). These matrix ele-

ments cannot be reliably calculated with an interaction that contains no density dependence, as evidenced by the fact that the giant monopole resonance [$s^{-1}sd$ and $p^{-1}pf$ particle-hole pairs coupled to $(\lambda,\mu)=(2,0)$] lies too low in energy. Secondly, the $(\lambda,\mu)=(2,0)$ part of the central interaction causes the 2p-4h (2,2) configurations and the $0\hbar\omega$ configurations to mix quite strongly so that the ground state is pushed down by several MeV. Of course, corresponding $4\hbar\omega$ configurations could be found which would push down the $2\hbar\omega$ configurations, but the increase in basis size would render the calculation intractable. (Reference 5 gives a detailed discussion of this problem.) In light of these difficulties and knowing that these configurations are of minor importance for the 0^+ to 2^+ transitions considered here, we have omitted the (2,2) representation. We shall comment further on this in our discussion of the ground state wave function.

We use the Cohen-Kurath (CK) (8–16)2BME interaction[3] for the p shell, and the Chung-Wildenthal (CW) interaction[13] for the sd shell. For the particle-hole interaction we use the Millener-Kurath (MK) interaction,[14] and all other two-body matrix elements are calculated from the same MK potential using harmonic oscillator single particle wave functions. The p-shell single particle energies are taken as the CK values, while those for the sd shell are fixed at the MK values.

The $0\hbar\omega$ and $2\hbar\omega$ intensities of the model wave functions for the 0^+ (g.s.) and first three 2^+ states are summarized in Table I. Admixtures of core excitations in the ground state are predicted to make up 8.4% of the wave function. This is to be compared with 4% predicted in the weak-coupling calculations of Lie,[4] and 17.2% predicted in the calculations of Kozub et al.[5] The factor of 2 difference in the ground state excitations between the latter calculation and the present work arises because, as discussed above, we have not included the $(\lambda,\mu)=(2,2)$ representation in our $2\hbar\omega$ basis and these configurations make up 14% of the g.s. wave function of Kozub et al.[5] It is, however, difficult to estimate reliably this percentage. The core-excitations in our ground state wave function have a dominant ^{12}C(0^+,g.s.)$\otimes^{18}$O(0^+,g.s.) structure similar to the 2p-4h components of Lie's wave function. The model wave function for the 0^+(6.59 MeV) level, which is mainly a $2\hbar\omega$ state, contains a sizable (13%) ^{12}C(2_1^+)$\otimes^{18}$O(2_1^+) component. A breakdown of the 0^+ and 2^+ wave functions according to SU(3) configuration is given in Table II.

The mixing between the lowest 2^+ states at 7.01 and 8.32 MeV is determined by the unperturbed energy position of the pure 2h and 2p-4h configurations and by the

TABLE I. $0\hbar\omega$ and $2\hbar\omega$ intensities in the 0^+ and 2^+ wave functions.

J_n^π	Lie (Ref. 4)		Kozub et al. (Ref. 5)		Present work	
	$0\hbar\omega$	$2\hbar\omega$	$0\hbar\omega$	$2\hbar\omega$	$0\hbar\omega$	$2\hbar\omega$
0_1^+	96	4	83	17	92	8
2_1^+	51	49			55	45
2_2^+	44	56			30	70
2_3^+	2	98			6	94

TABLE II. Intensities of SU(3) (λ,μ) representations for the 0^+(g.s.) and 2^+ wave functions of ^{14}C.

| (λ,μ) | $0\hbar\omega$ (s^4p^{10}) | | | | | $2\hbar\omega$ $[s^4p^8(sd)^2+s^4p^9(pf)]$ | | | | |
	(02)	(10)	(44)	(33)	(06)	(14)	(25)	(52)	(41)	(60)
J_n^π										
0_1^+	65.1	26.5	3.4	0.9	0.1	0.03	0.1	1.2	0.7	2.4
2_1^+	49.1	6.3	29.3	2.9	2.1	0.3	2.8	5.4	0.7	1.1
2_2^+	26.0	3.5	50.4	5.8	2.4	0.03	4.7	6.6	0.7	0.7
2_3^+	5.5	1.0	60.4	4.8	13.0	1.2	9.1	4.3	0.6	0.4

off diagonal $\langle p^2 | V | (sd)^2 \rangle$ matrix elements. Because these two states lie so close in energy, the $0\hbar\omega$ and $2\hbar\omega$ configuration mixing in the wave functions is very sensitive to the position of the centroids of the p shell and sd shell. As mentioned above, we have chosen to use the CK and MK values for these single particle energies. The 2_1^+(7.01 MeV) wave function involves 55.4% $0\hbar\omega$ excitation and the dominant core-excitations are 27% ^{12}C(0_1^+)$\otimes$^{18}O(2_1^+) and 16% ^{12}C(2_1^+)$\otimes$^{18}O(0_1^+). The 2_2^+(8.32 MeV) level, on the other hand, has a dominant (57%) ^{12}C(0_1^+)$\otimes$^{18}O(2_1^+) structure, while $0\hbar\omega$ excitations make up 30% of the wave function. The model wave functions for these 2^+ states correspond to a predicted energy splitting $\Delta E = E(2_2^+) - E(2_1^+) = 0.8$ MeV to be compared with the experimental value of 1.31 MeV. A similar underestimation is found in other shell model calculations (Ref. 4, for example). We note that Coulomb effects, which have not been included in the present calculations, decrease the experimental energy splitting of 1.31 MeV in ^{14}C to 1.26 MeV and 1.18 MeV in ^{14}N and ^{14}O, respectively. As the mixing between these two states is strongly sensitive to the magnitude of the energy splitting between them, it is possible that the structure of this 2^+ doublet varies from ^{14}C to ^{14}O.

The 2_3^+(10.45 MeV) level is predicted to have a dominant (93.5%) $2\hbar\omega$ structure; however, as will be discussed in Sec. III, the model wave function does not yield the observed (π,π') cross sections at this energy. At 10 MeV excitation $4\hbar\omega$ configurations are probably also important so that our $(0+2)\hbar\omega$ space may not allow for an adequate description of the 2_3^+ state. At 10.43 MeV there is also a state with a tentative 3^- spin and parity assignment,[8] which pion scattering would not resolve from the 2^+ state. A $1\hbar\omega$ shell model calculation, essentially similar to that of Ref. 14, has been carried out by Kurath[9] to describe the negative parity states of ^{14}C. The lowest 3^-(6.73 MeV) state is well described in this basis,[5] and the (π,π') data are reproduced.[12] However, the second and third 3^- states are predicted to lie at excitation energies of 10.7 and 13.5 MeV, respectively, i.e., at considerably higher energy than the 9.8 and 10.43 MeV levels. This may be a reflection of the need to include $3\hbar\omega$ excitations at these energies. In Sec. IV we discuss the fits of the second and third $1\hbar\omega$ 3^- wave functions to the (π,π') cross sections for the peak at 10.4 MeV.

III. DWIA ANALYSIS

A. Introduction

For comparison with the data we performed calculations in the distorted wave impulse approximation (DWIA) using the computer program ARPIN of Lee and Kurath.[15] The distorted waves were generated by the code PIPIT of Eisenstein and Tabakin.[16] For the proton point density we used a phenomenological shape which was derived from the ^{14}C charge density (obtained from elastic electron scattering) by unfolding the proton's charge distribution using the program ALLWORLD.[17] The neutron point distribution was assumed to scale with that for the protons by a factor of N/Z. The π-nucleus interaction was calculated by PIPIT from the π-nucleon phase shifts, 20 MeV below the actual π-nucleus center of mass energy. The Gaussian off-shell model option in PIPIT (Ref. 16) was used with $a_l = 3 \times 10^{-6}$ MeV^2 both for the $l = 0$ and $l = 1$ partial waves. The fit to the elastic data is very good with this parametrization (Fig. 1).

For the calculations of the inelastic cross sections we employed the transition densities derived using the one-body density matrix elements (OBDME's) from the shell model calculations discussed in Sec. II. As in previous analyses of inelastic pion scattering (Refs. 15, 18, and 19, for example), it was found necessary to introduce isoscalar and isovector polarization charges δ_0 and δ_1 or, equivalently, enhancement factors, $(1+\delta_0)$ and $(1+\delta_1)$, which multiply the shell model transition densities by a momentum-transfer independent factor. We use the convention of Ref. 19, $\delta_0 = \delta_p + \delta_n$ and $\delta_1 = \delta_p - \delta_n$. The polarization charges were applied only to the dominant $\Delta S = 0$ densities, i.e., those which do not involve a spin transfer to the target. In addition, only those OBDME's corresponding to transitions within the p shell or sd shell were enhanced, while transitions of the type $0p \rightarrow 1p0f$ were not. These latter transitions are weak and contribute very little to the pion cross sections.

B. The 2_1^+(7.01 MeV) state

We first consider the excitation of the 2_1^+(7.01 MeV) level. Assuming reasonable polarization charges, $\delta_n = \delta_p = 0.35$, with our oscillator parameter $b = 1.7$ fm,
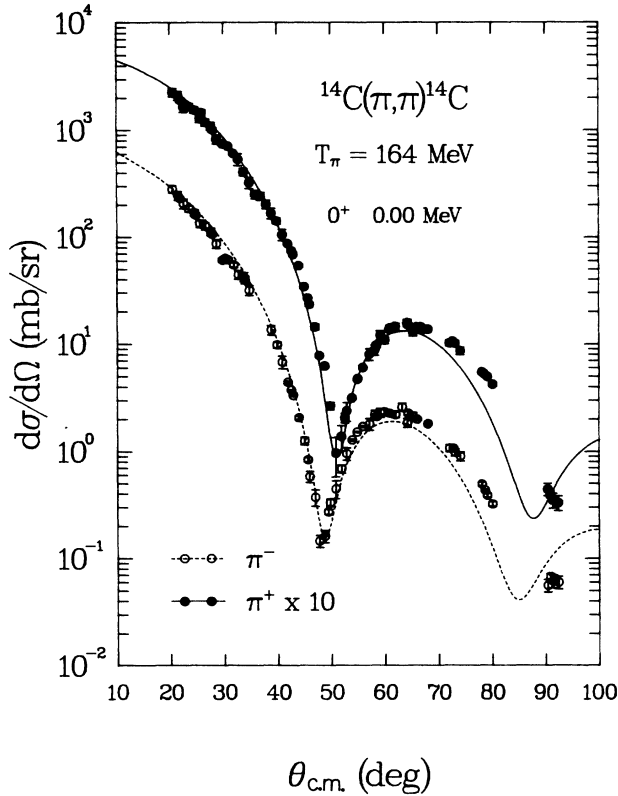
FIG. 1. Differential cross sections for π^+ and π^- elastic scattering from ^{14}C at $T_\pi = 164$ MeV. The solid and dashed lines were calculated with PIPIT using a ground state density derived from electron scattering.
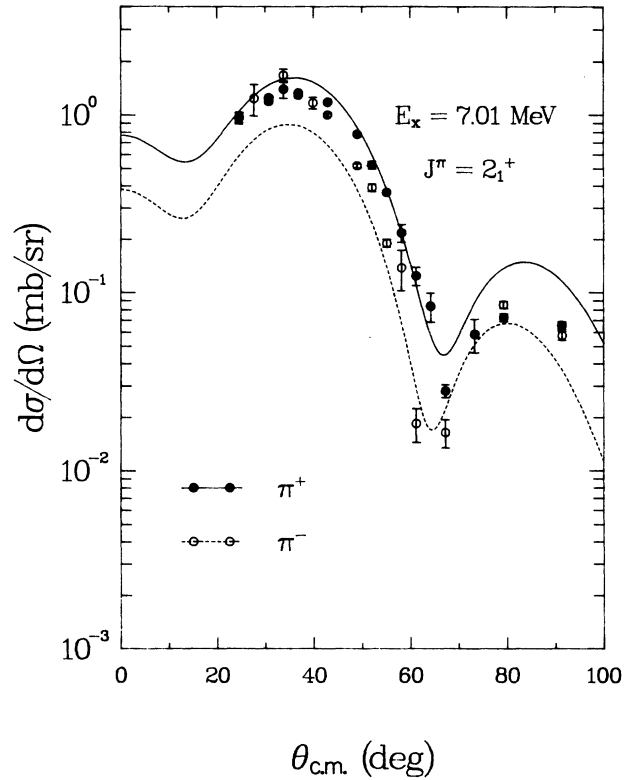
FIG. 2. Differential cross sections for ^{14}C$(\pi,\pi')^{14}$C$(2^+,7.01$ MeV) at $T_\pi = 164$ MeV. The solid and dashed lines were calculated with ARPIN using shell model OBDME's with effective charges $1+\delta_0 = 1.7$ and $1+\delta_1 = 1.0$.

the predicted angular distributions are shown in Fig. 2. Clearly, the shapes of the distributions and the magnitude of the π^+ cross section are quite well reproduced. However, the π^- cross section is underpredicted by almost a factor of 2. Remarkably, the experiment shows near equality between the π^+ and π^- cross sections. Since the g.s. wave function contains only 8.4% core excitation this $0_1^+ \rightarrow 2_1^+$ transition remains proton dominated in our extended $(0+2)\hbar\omega$ shell model calculations, so that a ratio $\sigma(\pi^+)/\sigma(\pi^-) \simeq 1$ is difficult to understand. The severe constraints which this result places on theory is illustrated by the following approximate formulae for the peak cross sections:

$$d\sigma/d\Omega(34°,\pi^+) = [0.64(1+\delta_0) + 0.12(1+\delta_1)]^2 , \qquad (1)$$

$$d\sigma/d\Omega(34°,\pi^-) = [0.61(1+\delta_0) - 0.11(1+\delta_1)]^2 . \qquad (2)$$

Here the coefficients 0.64, 0.12, etc. are the cross section amplitudes in $(mb/sr)^{1/2}$ calculated with ARPIN (Ref. 15) using the shell model transition densities of this work. We note that the coefficients in (1) are slightly larger than those in (2) which results from Coulomb effects. The isovector terms enter with opposite sign in the two cases as expected at incident pion energies near the [3,3] pion-nucleon resonance.

If we assume that $\delta_p \simeq \delta_n$, Eqs. (1) and (2) imply a cross section for π^+ which is significantly larger than for π^-, in contradiction to the data. The schematic calculations of Ref. 6 show the same feature. One method of reproducing the data is to choose an isovector effective charge $1+\delta_1 \leq 0$. This, however implies $\delta_n \geq 1+\delta_p$, which is unreasonable. Another possibility is to arbitrarily increase the intensity of the $p^{-4}(sd)^2$ configurations in the ground state in order to obtain equal neutron and proton contributions to the transition amplitude. This, however, would require $2\hbar\omega$ configurations to dominate the g.s. wave function, which is unphysical. Use of a dominating $p^{-4}(sd)^2$ component also has the effect of changing the shape of the angular distribution so that there is no longer agreement with the data.

In order to fit the near equality of the π^+ and π^- data and the angular distribution shapes it is necessary that the isovector contribution be small. Ideally, it should be slightly negative in Eq. (1) and positive in Eq. (2). This can be achieved by adopting different polarization charges for the p and sd shells. We rewrite Eqs. (1) and (2) using the p- and sd-shell cross section amplitudes explicitly, i.e.,

$$d\sigma/d\Omega(34°,\pi^+) = \{0.51[1+\delta_0(p)]+0.13[1+\delta_0(sd)]+0.18[1+\delta_1(p)]-0.06[1+\delta_1(sd)]\}^2 \,, \tag{3}$$

$$d\sigma/d\Omega(34°,\pi^-) = \{0.48[1+\delta_0(p)]+0.13[1+\delta_0(sd)]-0.17[1+\delta_1(p)]+0.06[1+\delta_1(sd)]\}^2 \,. \tag{4}$$

We thus have four parameters $\delta_0(p)$, $\delta_0(sd)$, $\delta_1(p)$, and $\delta_1(sd)$, and we take some guidance from other data to estimate their values.

We first consider the sd shell. From the dominantly single particle levels of ^{17}O and ^{17}F, we can deduce proton and neutron effective charges. Using the $(0+2)\hbar\omega$ wave functions of Ellis and Engeland[20] and our oscillator parameter, $b=1.7$ fm, the ground state quadrupole moments[21] of these nuclei give[22] $\delta_n(sd)=0.43\pm0.06$ and $1+\delta_p(sd)=1.86\pm0.37$ for the $d_{5/2}\rightarrow d_{5/2}$ amplitude. [The $B(E2:\frac{1}{2}^+\rightarrow\frac{5}{2}^+)$ data yield similar polarization charges for the $d_{5/2}\rightarrow s_{1/2}$ amplitude: namely, $\delta_n(sd)=0.44\pm0.003$ and $1+\delta_p(sd)=1.89\pm0.03$.] It is unwise to accept the proton charge at face value as the weak proton binding energy of only 0.6 MeV in ^{17}F will cause the the $d_{5/2}$ wave function to have an unusually long tail, and correspondingly large $\langle r^2 \rangle$ matrix element. For the 2_1^+ state in ^{14}C a larger binding energy, close to 4.0 MeV, is probably a more reasonable value. We therefore add to $1+\delta_p$ the difference in $\langle r^2 \rangle$ obtained with Woods-Saxon wave functions bound by 4.0 and 0.6 MeV, respectively, divided by the oscillator value of $\langle r^2 \rangle$. With the standard Woods-Saxon well parameters of Ref. 23, we obtain $\delta_p(sd)=0.71$. Thus, from the mass 17 data we derive effective charges $1+\delta_0(sd)=2.14$ and $1+\delta_1(sd)=1.28$.

It is interesting to compare these effective charges with those needed for the $0_1^+\rightarrow 2_1^+$ transitions in mass 18. We used the $(0+2)\hbar\omega$ wave functions of Ref. 24 to describe the $J^\pi=0^+$ and 2^+ states. The peak cross sections[19] for π^+ and π^- inelastic excitation of the 1.98 MeV 2^+ level in ^{18}O were fitted as a function of the isoscalar and isovector effective charges. Figure 3 summarizes these results. In this plot each line represents the set of $1+\delta_0$ and $1+\delta_1$ values which reproduce the experimental value of the labeled observable, and the width of the line corresponds to the experimental uncertainties in that observable. Lines corresponding to the π^+ cross sections have opposite slope to those for the π^- cross sections because the isoscalar and isovector amplitudes appear with opposite relative signs in the two cases at energies near the [3,3] resonance. We have also fitted the $B(E2:2_1^+\rightarrow 0_1^+)$ data[21] for ^{18}O and ^{18}Ne (Fig. 3). The four curves intersect approximately at the point with coordinates of $1+\delta_0\simeq2.2$ and $1+\delta_1\simeq1.3$, which are close to the values deduced from mass 17. We therefore adopt these latter effective charges for the sd shell, namely, $1+\delta_0=2.14$ and $1+\delta_1=1.28$.

To obtain effective charges for the p shell we studied the dominantly single-hole $\frac{1}{2}^-$(g.s.) and $\frac{3}{2}^-$(6.23 MeV) states of ^{15}N. We carried out a $(0+2)\hbar\omega$ shell model calculation in which spurious c.m. motion was exactly eliminated. The two-body interaction and single particle energies were the same as those in our shell model calcula-

tions for ^{14}C (Sec. II). The intensities of $2\hbar\omega$ configurations, principally 2p-3h, are 7.6% and 11.4% for the $\frac{1}{2}^-$ and $\frac{3}{2}^-$ levels, respectively. We fitted the $\sigma(\pi^+)/\sigma(\pi^-)$ cross-section ratio[25] for excitation of the $\frac{3}{2}^-$ level and the $B(E2:\frac{1}{2}^-\rightarrow\frac{3}{2}^-)$ value to determine proton and neutron effective charges. This analysis yields $1+\delta_0=2.08$ and $1+\delta_1=0.35$ or, equivalently, $\delta_p=0.22$ and $\delta_n=0.87$. The need for a large neutron effective charge arises because the observed cross-section ratio $\sigma(\pi^+)/\sigma(\pi^-)$ is only 1.5, whereas for proton hole states we expect the π^+ cross sections to be roughly 9 times larger than the π^- cross sections. To reproduce the observed π^+/π^- ratio it is necessary to quench strongly the isovector amplitudes. This is consistent with the suggestion of Poletti *et al.*[26] that $1+\delta_0 \gg 1+\delta_1$ is needed to explain the near equality in magnitude of the $E2/M1$ mixing ratios for the $3/2_1^-\rightarrow1/2_1^-$ transition in ^{15}N and ^{15}O.

A similar analysis can be applied to the strong $\Delta J=2$ transitions in ^{13}C. From the (e,e') form factor and the π^+/π^- cross-section ratio for the excitation of the $\frac{5}{2}^-$(7.55 MeV) level, Millener[27] extracts the values $1+\delta_0=1.61$ and $1+\delta_1=0.68$. These latter values correspond to a smaller neutron effective charge than that derived from the ^{15}N data. For our present study of the 2^+ states in ^{14}C we chose values for the effective charges intermediate between those for $A=13$ and $A=15$. We took some guidance from Eqs. (3) and (4) and chose effective charges of $1+\delta_0(p)=1.8$ and $1+\delta_1(p)=0.4$. These values are consistent with the data for nuclei at the end of the p shell but cannot be viewed as definitive.
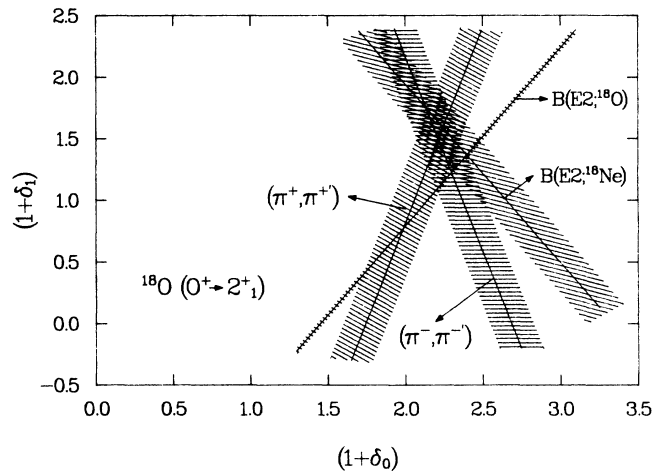

FIG. 3. Constraints on $(1+\delta_0)$ and $(1+\delta_1)$ implied by the observed $B(E2:0_1^+\rightarrow2_1^+)$ values in ^{18}O and ^{18}Ne and the ^{18}O$(\pi,\pi')^{18}$O$(2^+,1.98$ MeV) cross section data. The transition densities used were derived from a $(0+2)\hbar\omega$ shell model calculation.

The most obvious difference between these p-shell values and those derived from the data for the sd-shell nuclei ^{17}O, ^{17}F, ^{18}O, and ^{18}Ne is the change in $1+\delta_1$ from 1.28 to 0.4. The differences in effective charges between the p shell and the sd shell are, however, reasonable. Neutron and proton polarization charges for the ^{16}O region have been studied[22] in various elaborate perturbation-theoretic calculations and the values for the p shell are generally found to be larger than those obtained for the sd shell. This difference is of most significance for neutrons giving us a large value of $\delta_n(p)$. In the case of protons, the weak binding energy for the sd shell leads to a significant enhancement in $\langle r^2 \rangle$ compared to the oscillator value, and hence to a large proton effective charge close to the closed shell. As one moves towards the middle of the sd shell these binding energy effects are no longer important and Brown et al.[28] used values of $1+\delta_0 = 1.7$ and $1+\delta_1 = 1.0$ in their analysis of effective charges for the entire sd shell.

Using the values of the effective charges which we have discussed above, the DWIA produces the angular distributions for π^+ and π^- excitation of the 7.01 MeV 2_1^+ in ^{14}C shown in Fig. 4. Clearly both the shapes and the magnitudes of the predictions compare quite well with the data. In particular the predicted magnitude of the forward peak for π^+ is only 4% larger than for π^-, which is within the limits imposed by the data.

C. The $B(E2:2_1^+ \rightarrow 0_1^+)$ data

In ^{14}C and ^{14}O the electromagnetic transitions $2_1^+(T=1) \rightarrow 0_1^+(T=1)$ contain both isoscalar and isovector contributions appearing with opposite relative signs in the two nuclei, whereas the analog transition in ^{14}N involves only an isoscalar term. In a pure p-shell calculation the isoscalar and isovector matrix elements are equal in magnitude so that without effective charges we obtain a ratio $B(E2;^{14}\text{C}):B(E2;^{14}\text{N}):B(E2;^{14}\text{O})=4:1:0$. Allowing excitations to higher shells results in an isovector matrix element which is reduced with respect to the isoscalar matrix element leading to a smaller predicted value for
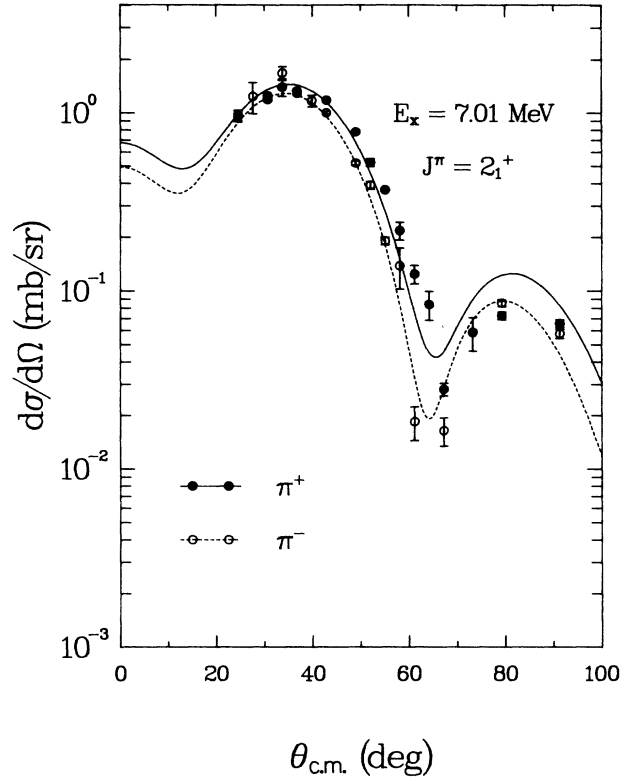

FIG. 4. The same as Fig. 2, but with shell dependent effective charges $1+\delta_0(p)=1.8$, $1+\delta_1(p)=0.4$, $1+\delta_0(sd)=2.14$, and $1+\delta_1(sd)=1.28$.

the ratio $B(E2;^{14}\text{C})/B(E2;^{14}\text{N})$ and a nonzero $B(E2)$ strength for the analog transition in ^{14}O. Table III lists these transition strengths together with the experimental values.[21,29] The $B(E2:2_1^+ \rightarrow 0_1^+)$ in ^{14}C is reproduced without effective charges, but in this case the corresponding transition in ^{14}N is underestimated by almost a factor of 3. When standard effective charges,[28] $1+\delta_0 = 1.7$ and $1+\delta_1 = 1.0$, which reproduce the π^+ (but not the π^-)

TABLE III. Transition Strengths for the 2^+ $T=1$ levels to the 0_1^+ $T=1$ level in $A=14$. All $B(E2)$ values are quoted in Weisskopf units. The radial matrix elements were evaluated using harmonic oscillator wave functions with oscillator parameter $b=1.7$ fm.

	$E_i \rightarrow E_f$ (MeV)	Expt.	Theory[a]	Theory[b]	Theory[c]
^{14}C	$7.01 \rightarrow 0.0$	1.8 ± 0.3[d]	1.84	4.1	3.1
	$8.32 \rightarrow 0.0$	0.39 ± 0.15[d]	0.71	0.82	0.4
^{14}N	$9.17 \rightarrow 2.31$	2.5 ± 0.3[e]	0.93	2.7	3.1
	$10.43 \rightarrow 2.31$		0.01	0.02	0.01
^{14}O	$6.56 \rightarrow 0.0$		0.33	1.57	3.1
	$7.77 \rightarrow 0.0$		0.45	0.37	0.16

[a]No effective charges $1+\delta_0 = 1.0$, $1+\delta_1 = 1.0$.
[b]Standard effective charges $1+\delta_0 = 1.7$, $1+\delta_1 = 1.0$.
[c]Shell dependent effective charges $1+\delta_0(p)=1.8$, $1+\delta_1(p)=0.4$, $1+\delta_0(sd)=2.1$, $1+\delta_1(sd)=1.2$.
[d]From the (e,e') data of Ref. 29.
[e]Reference 21.

cross section to the 2_1^+ state are used, the transition strength in ^{14}N is correct, but that in ^{14}C is overestimated by more than a factor of 2. If we use the shell-dependent effective charges necessary to explain the π^+/π^- ratio the agreement between experiment and theory is considerably improved, although the predicted value for the 2_1^+ state in ^{14}C is still too large. These effective charges cause the isovector matrix element to become negligibly small so that the predicted $2_1^+ \rightarrow 0_1^+$ strength is the same for all three nuclei. The fact that the strength of the $2_1^+(T=1) \rightarrow 0_1^+(T=1)$ transition is observed to be larger in ^{14}N than in ^{14}C is quite surprising. An extensive measurement of the longitudinal (e,e') form factor for this $2_1^+(7.01$ MeV) state would be very valuable. A measurement of the analog transition in ^{14}O (if experimentally feasible) would provide a crucial test of the isovector versus isoscalar nature of these transitions.

D. The $2_2^+(8.32$ MeV) state

The DWIA predictions for the $2_2^+(8.32$ MeV) level using shell independent effective charges, $1+\delta_0=1.7$, $1+\delta_1=1.0$, are shown in Fig. 5. The shape of the π^+ angular distribution agrees quite well with experiment but the magnitude is too small by a factor of 2. The π^- cross section is also underpredicted insofar as the large experimental uncertainties permit a determination. We note that at several angles only upper limits could be extracted

for the π^- cross section. The lack of any observable cross section at these angles is illustrative of the strong cancellation between neutron (*sd*-shell) and proton (*p*-shell) components in the transition. This destructive interference is also seen in the π^+ data where the cross section is an order of magnitude smaller than for the 2_1^+ state.

In Fig. 6 we show the predicted cross sections using the shell-dependent effective charges discussed above. The π^+ cross-section magnitude is reduced slightly, but the shape of the angular distribution agrees well with the data. The π^- data is quite well reproduced in general magnitude with the use of these effective charges, but the cross section appears to have too little structure, although the data are not definitive on this point.

The strong destructive interference between the *p*-shell and *sd*-shell contributions to the transition amplitudes causes the DWIA predictions for the π^+ and π^- cross sections for this 2_2^+ state to be very sensitive to small components in the wave functions of the 0_1^+ and 2_2^+ states. For example, the OBDME's involving the $d_{3/2}$ level are relatively small; however, if we omit these transition amplitudes the DWIA prediction for the π^+ cross section increases considerably, and the shape of the π^- angular distribution is changed. The predicted π^+ and π^- cross sections also show strong sensitivity to small changes in the distorted waves. This contrasts with the strong transition to the $2_1^+(7.01$ MeV) state where the DWIA predictions remain stable with respect to small changes in the shell model wave functions or the distort-
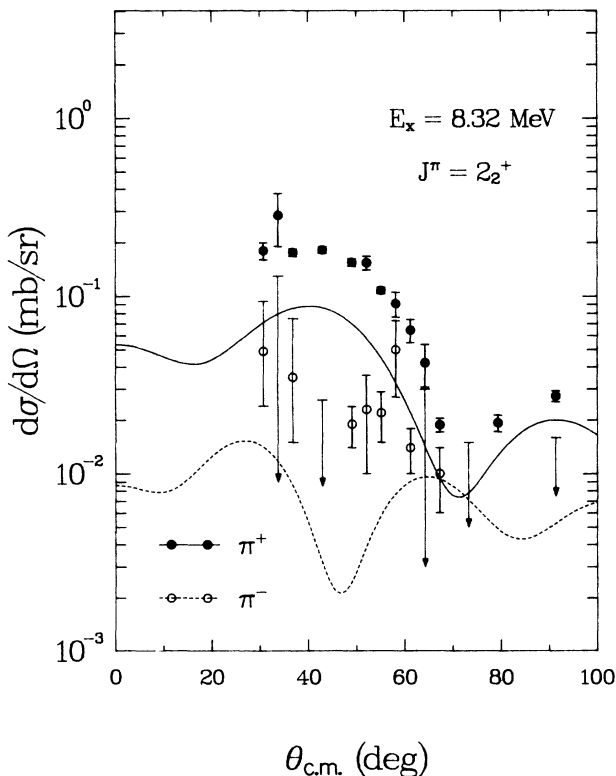

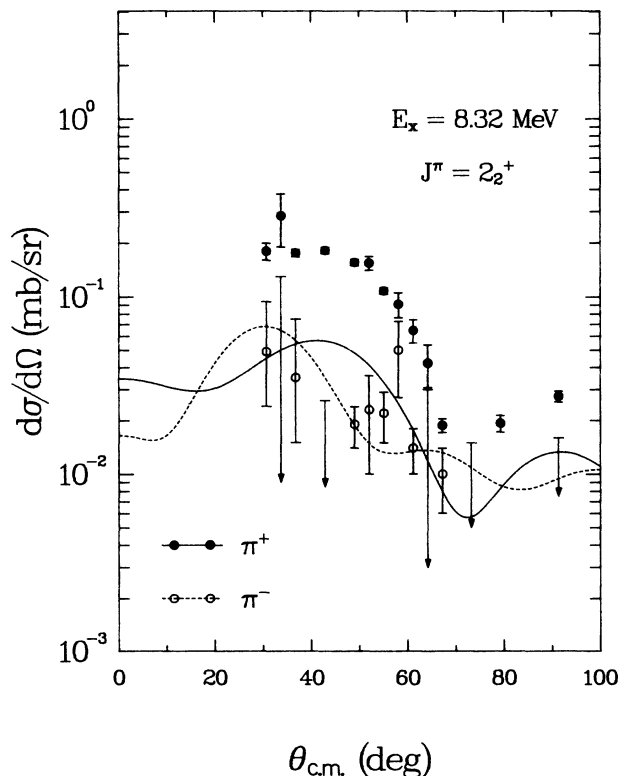FIG. 5. The same as Fig. 2 but for the $2^+(8.32$ MeV) state.

FIG. 6. The same as Fig. 5, but with shell dependent effective charges as in Fig. 4.

ed waves. Because of the sensitivity of the 2_2^+ cross sections to details of the calculations it is difficult to draw definite conclusions regarding the structure of this state from the (π,π') data. However, it is clear that the wave function involves a strong mixing of the p^{-2} and $p^{-4}(sd)^2$ configurations.

In Refs. 6 and 7 schematic weak-coupling model calculations were reported in which the two 2^+ states at 7.01 and 8.32 MeV were assumed to be equal admixtures of p^{-2} and $p^{-4}(sd)^2$ configurations. The intensity of the $p^{-4}(sd)^2$ configurations in the ground state was then adjusted to give the best fit to the (π,π') data, and this optimal value corresponded to 19% g.s. core excitation. If we arbitrarily adjust the intensity of the $2\hbar\omega$ admixture in the ground state to 19% in the present model, we find the predicted shape of the angular distributions for the (π,π') data to the $2^+(8.32$ MeV) state to be in strong disagreement with the data. Thus, the present calculations are not in agreement with the suggestion of 19% (or more) core excitation in the ground state of ^{14}C, but, of course, smaller variations from our model value of 8.4% are not ruled out. It is interesting to note that Fortune and Stephans[30] obtain a core excitation intensity of 12% from a study of their (t,p) data.

E. Coupled-channel calculations

Finally, in our study of this 2^+ doublet it is important to examine coupled-channel (CC) effects. Couplings between the three states $(0_1^+, 2_1^+, 2_2^+)$ were calculated using the momentum space coupled-channel computer code SHOCK.[31] A consistent set of transition densities derived from the shell model calculations (Sec. II) was used, together with our shell-dependent effective charges. It was found that for the $2_1^+ \rightarrow 2_2^+$ transition only the $\Delta J=0$ and $\Delta J=2$ amplitudes were significant and hence all other ΔJ values were omitted. The resulting angular distributions for the excitation of the 2_1^+ and 2_2^+ states are shown in Figs. 7 and 8, respectively. For the 2_1^+ state there is a small enhancement in the cross section at forward angles and both the π^+ and π^- predictions remain in good agreement with the data. In the case of the 2_2^+ state, the shape of the CC π^+ angular distribution differs somewhat from the DWIA prediction. The cross section is enhanced, but the calculation still underestimates the data by about a factor of 3. The large change in the shape of the π^- angular distribution reflects the very strong sensitivity of this weak transition to the model used. In light of these sensitivities we regard the comparison between the predicted and the experimental π^- cross sections as reasonable. However, the model clearly gives too much destructive interference between the p-shell and sd-shell amplitudes for the $(\pi^+,\pi^{+'})$ data.

F. The peak at 10.4 MeV

In Fig. 9 we show a comparison between the observed (π,π') angular distribution for the peak at 10.4 MeV and the DWIA predictions for the $2_3^+(10.45$ MeV) state. In this calculation we have used shell independent effective charges $1+\delta_0=1.7$, $1+\delta_1=1.0$. Clearly, the model

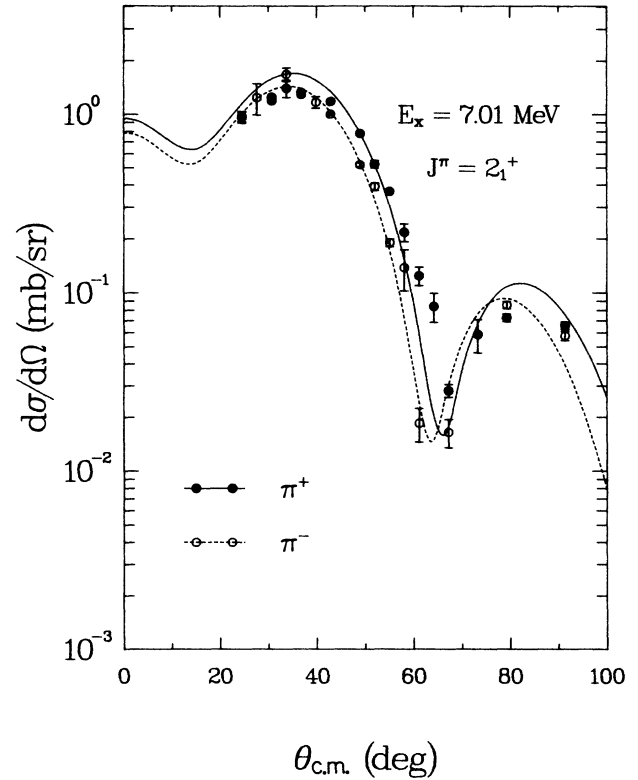FIG. 7. Differential cross sections for $^{14}C(\pi,\pi')^{14}C(2^+,7.01$ MeV) at $T_\pi=164$ MeV obtained from $(0_1^+,2_1^+,2_2^+)$ CC calculations.
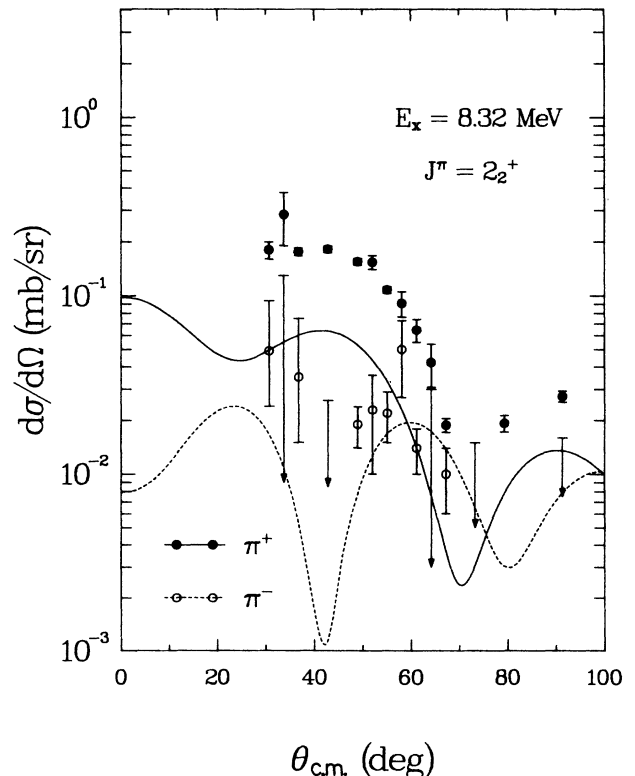

FIG. 8. The same as Fig. 7, but for the $(2^+,8.32$ MeV) state.

wave function fails in predicting the π^+ and π^- cross-section magnitudes and gives a poor fit to the shape of the angular distributions. In addition, the π^+ cross section is predicted to be larger than the π^- cross section, in contradiction to the data. The small magnitude of the cross section for the model $0_1^+ \rightarrow 2_3^+$ transition can be understood as a consequence of the relatively small (8.4%) admixture of $p^{-4}(sd)^2$ configurations in the g.s. wave function and the dominant (93.5%) $2\hbar\omega$ structure of the 2_3^+ state. As discussed in Sec. II, $4\hbar\omega$ configurations may be important for an adequate description of this 2_3^+ state. However, $4\hbar\omega$ excitations are unlikely to make up a large fraction of the g.s. wave function, so that no significant increase is expected in the magnitude of the DWIA cross sections for the $0_1^+ \rightarrow 2_3^+$ transition. This suggests that the $3_3^-(10.43$ MeV) state and/or the $\geq 1(10.5$ MeV) state contribute most of the observed cross section at 10.4 MeV. Figure 9 shows the DWIA predictions for the 3_2^- theoretical state predicted at 10.7 MeV, and it is clear that the model predictions using $1+\delta_0 = 1.5$ and $1+\delta_1 = 1.0$ agree reasonably well with the data. The 3_3^- theoretical state is predicted to lie at 13.5 MeV of excitation, and the π^+ angular distribution for this state is very similar in shape and magnitude to that for the 3_2^- state. However, the π^- cross section for the model 3_3^- state under predicts the data by almost a factor of 3. Since, in Fig. 9, we are comparing predictions for the second theoretical 3^- level with the data for the third experimental 3^- state, we caution against drawing definite con-

clusions and emphasize the possible need to include $3\hbar\omega$ states at this excitation energy. However, the data are consistent with a $\Delta L = 3$, $\Delta S = 0$ transition to a 3^- state.

IV. CONCLUSIONS

The inelastic pion data on ^{14}C show near equality of the π^+ and π^- cross sections for the $2_1^+(7.01$ MeV) state and strong cancellations between the neutron and proton amplitudes for the second 2^+ state. The $B(E2)$ value for the $2_1^+ \rightarrow 0_1^+$ transition in ^{14}C is smaller than for the analog transition in ^{14}N, which is quite unexpected. In order to interpret these data we have carried out large scale $(0+2)\hbar\omega$ shell model calculations in an SU(3) basis for the nucleus ^{14}C. The transition amplitudes required effective charge enhancement in order to explain the pion and $B(E2)$ data. For the $(sd) \rightarrow (sd)$ amplitudes we used effective charges deduced from the mass 17 and 18 data, while for the $p \rightarrow p$ amplitudes we used values intermediate between those obtained from the mass 13 and 15 data. The principal difference from a conventional shell-independent choice was that the proton charge for the weakly bound (sd) levels had to be strongly enhanced with respect to our chosen oscillator basis.

Our effective charges led to a strong quenching of the isovector component of the $0_1^+ \rightarrow 2_1^+$ transition which was necessary to explain the π^+/π^- cross-section ratio; a similar requirement was evident from a comparison of the ^{14}C and ^{14}N $B(E2)$ data. The $0_1^+ \rightarrow 2_2^+$ transition, which showed strong cancellations between the contributions from the p^{-2} and $p^{-4}(sd)^2$ configurations, was sensitive to details of the calculations. In this case our calculated $B(E2)$ value was in good agreement with experiment. For the pion scattering it was necessary to include multistep processes involving the 2_1^+ level in a coupled-channel calculation, but the magnitude of the predicted π^+ cross section remained too small.

We also examined inelastic scattering data to a group of levels at 10.4 MeV with spins of (3^-), 2^+, and ≥ 1. The cross sections obtained for the 2_3^+ level were much smaller than the data; however, the observed shape was consistent with a $\Delta L = 3$, $\Delta S = 0$ transition.

Again we emphasize the importance of further measurements of the $2^+(T=1) \rightarrow 0^+(T=1)$ transition strengths in the $A = 14$ nuclei. In particular, extensive measurements of the longitudinal (e,e') form factors to the 2^+ states in ^{14}C would be most valuable. In addition, a study of the analog transitions in ^{14}O (if experimentally feasible) would provide a less ambiguous determination of the isoscalar versus isovector contributions to these transitions.
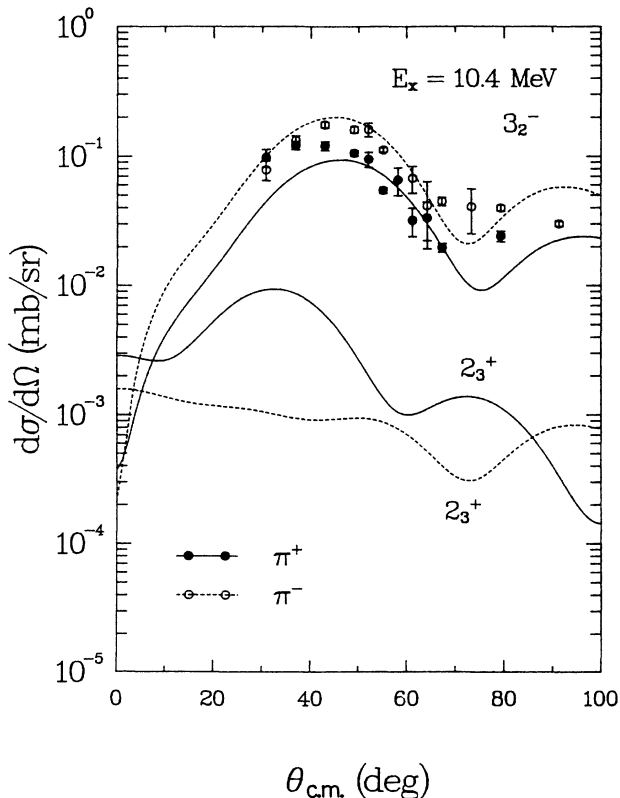

FIG. 9. Differential cross sections for ^{14}C$(\pi,\pi')^{14}$C at 10.4 MeV of excitation. The curves were obtained from ARPIN using the shell model transition densities for the 2_3^+ and 3_2^- states.

*Present address: Department of Physics, California State Polytechnic University, Pomona, CA 91768.

†Present address: Los Alamos National Laboratory, Los Alamos, NM 87545.

‡Present address: Fermi National Accelerator Laboratory, Batavia, IL 60510.

[1]I. Unna and I. Talmi, Phys. Rev. **112**, 452 (1958).

[2]E. K. Warburton and W. T. Pinkston, Phys. Rev. **118**, 733 (1960).

[3]S. Cohen and D. Kurath, Nucl. Phys. **73**, 1 (1965).

[4]S. Lie, Nucl. Phys. **A181**, 517 (1972).

[5]R. L. Kozub, J. Lin, J. F. Mateja, C. J. Lister, D. J. Millener, and E. K. Warburton, Phys. Rev. C **23**, 1571 (1981).

[6]D. B. Holtkamp, S. J. Seestrom-Morris, S. Chakravarti, D. Dehnhard, H. W. Baer, C. L. Morris, S. J. Greene, and C. J. Harvey, Phys. Rev. Lett. **47**, 216 (1981).

[7]D. Dehnhard, Nucl. Phys. **A374**, 377c (1982).

[8]R. O. Lane, H. D. Knox, P. Hoffmann-Pinther, R. M. White, and G. F. Auchampaugh, Phys. Rev. C **23**, 1883 (1981).

[9]D. Kurath, private communication.

[10]H. A. Thiessen and S. Sobottka, Los Alamos National Laboratory Report LA-4534-MS, 1970 (unpublished).

[11]C. J. Harvey, H. W. Baer, J. A. Johnstone, C. L. Morris, S. J. Seestrom-Morris, D. Dehnhard, D. B. Holtkamp, and S. J. Greene, Phys. Rev. C **33**, 1454 (1986).

[12]D. B. Holtkamp, S. J. Seestrom-Morris, D. Dehnhard, H. W. Baer, C. L. Morris, S. J. Greene, C. J. Harvey, D. Kurath, and J. A. Carr, Phys. Rev. C **31**, 957 (1985).

[13]W. Chung, Ph.D. thesis, Michigan State University, 1976 (unpublished).

[14]D. J. Millener and D. Kurath, Nucl. Phys. **A255**, 315 (1975).

[15]T.-S. H. Lee and D. Kurath, Phys. Rev. C **21**, 293 (1980).

[16]R. A. Eisenstein and F. Tabakin, Comput. Phys. Commun. **12**, 237 (1976).

[17]J. A. Carr, F. Petrovich, D. Halderson, and J. J. Kelly, code ALLWORLD (unpublished), and M. A. Franey, private communication.

[18]T.-S. H. Lee and R. D. Lawson, Phys. Rev. C **21**, 679 (1980).

[19]S. Chakravarti, D. Dehnhard, M. A. Franey, S. J. Seestrom-Morris, D. B. Holtkamp, C. L. Blilie, A. C. Hayes, C. L. Morris, and D. J. Millener, Phys. Rev. C **35**, 2197 (1987).

[20]P. J. Ellis and T. Engeland, Nucl. Phys. **A144**, 161 (1970).

[21]F. Ajzenberg-Selove, Nucl. Phys. **A460**, 1 (1986); **A392**, 1 (1983).

[22]F. L. Goodin and P. J. Ellis, Nucl. Phys. **A334**, 229 (1980); S. Chakravarti, P. J. Ellis, T. T. S. Kuo, and E. Osnes, Phys. Lett. **109B**, 141 (1982).

[23]S. Siegel, Ph.D. thesis, Rutgers University, 1970 (unpublished).

[24]A. C. Hayes, Ph.D. thesis, Yale University, 1986 (unpublished); A. C. Hayes, D. A. Bromley, and D. J. Millener (unpublished).

[25]D. P. Saunders, M. S. thesis, University of Texas, 1984.

[26]A. R. Poletti, E. K. Warburton, and D. Kurath, Phys. Rev. **155**, 1096 (1967).

[27]D. J. Millener, in *Pion-Nucleus Physics: Future Directions and New Facilities at LAMPF*, AIP Conf. Proc. No. 163, edited by R. J. Peterson and D. D. Strottman (AIP, New York, 1988), p. 402.

[28]B. A. Brown, B. H. Wildenthal, W. Chung, S. E. Massen, M. Bernas, A. M. Bernstein, R. Miskimen, V. R. Brown, and V. A. Madsen, Phys. Rev. C **26**, 2247 (1982).

[29]H. Crannell, P. L. Hallowell, T. J. O'Brien, J. M. Finn, and F. J. Kline, in *Proceedings of the International Conference on Nuclear Structure Studies using Electron Scattering and Photoreaction*, Sendai, Japan, 1972, edited by K. Shoda and H. Ui (Tohuku University, Sendai, 1972), p. 375.

[30]H. T. Fortune and G. S. Stephans, Phys. Rev. C **25**, 1 (1982).

[31]S. Chakravarti, Phys. Lett. **90B**, 350 (1980).